Experimental critical analysis of plate impedance

C. V. D´Alkaine[1]*, G. A. de Oliveira Brito[1], C. M. Garcia[2], P. R. Impinnisi[2]

[1] *Group of Electrochemistry and Polymers, Chemistry Department, Federal University of São Carlos,*
R. Washington Luiz Km 234, CEP 13560-905, São Carlos (SP), Brazil
[2] *Batteries Laboratory, Institute of Technology for Development-LACTEC, UFPR Polytechnic Centre,*
POBox 19067, CEP 81531-980, Curitiba (PR), Brazil

Taking into account that there are no experimental proofs that Electrochemical Impedance Spectroscopy (EIS) four electrode plate cell measurements can be attributed only to the central plate, in the present work measurements with variable counter-electrode plate areas and one and the same central plate were made. This was done in a frequency range from 10^4 to 10^{-2} Hz and at different central plate states of charge. The results show that for positive-negative-positive plate ensembles, at all studied frequencies and state of discharge, the EIS data can be attributed to the central negative plate, except for the highest counter-electrode/central working electrode areas ratio, r, and higher discharge levels, at the lower studied frequencies. Instead of that, for negative-positive-negative ensembles, the EIS data can be attributed to the central positive plate only at the high and middle studied frequencies in all discharge levels and area ratios. Totally charged central positive plates must be excluded because their impedance depends on the counter-electrode area at all r ratios. All these results are discussed and suppositions are made for their interpretation.

Key words: electrochemical impedance spectroscopy, four electrode EIS method, single plate EIS, counter-electrode variable area, lead acid battery plate EIS.

1. INTRODUCTION

The Electrochemical Impedance Spectroscopy (EIS) of porous electrodes has been studied theoretically [1–7] and experimentally [6–12]. From theoretical point of view, most of the models have been based on one pore model EIS [1], sometimes not taking into account the surface in which the pore is present. From experimental point of view, there are results on many different pores structures, going from simple roughness surfaces [6] to the most varied real porous electrodes [6–12].

Theoretical work on a single pore has shown that EIS depends on the pore shape, if this is located on a conductive metal surface [2]. At low frequencies, the theoretical EIS tends to show a simple capacity behavior (a straight line perpendicular to real axis, in Nyquist's plot). This straight line gives at the real axis, by extrapolation, something near to an average resistance of the inner solution inside the pore. Nevertheless, the equations without extrapolation at middle and high frequencies, due to different inner solutions resistances for each pore surface region, give EIS values shifted to the left in Nyquist's plot. This is because there is a.c. current distribution, due to these resistance differences. They give rise to a lower real impedance component, which produces a shift to the left of simple capacity behavior at low frequencies. This fact can even give rise to a partial capacity loop, followed at low frequencies by the capacity behavior, when the pore has a geometrical drop shape [2].

The experimental data with flat metal electrodes [13] give results, which seem to indicate one constant phase angle component. In contrast to that, powder metal electrodes seem to give two different phase angles components, at two different frequency ranges [8].

Considering EIS experimental data from real porous systems, the simple capacity behavior has never been observed. In general, EIS plots of real porous systems [6–12, 14] present inductive loops at very high and low frequencies. In the middle frequency range, they can have one or more capacity loops. The observed structures are different in different frequency ranges because the current related to the perturbation will go deeply inside the porous structure when the frequency is reduced [9, 10]. This is valid only for electrode materials, which have reasonable electronic conductance.

In the specific case of lead acid batteries EIS measurements, several papers have been published on batteries "as received" from factory [14–18]. On the other hand, papers have been published on open batteries. This permits access to the plates and introducing a reference electrode [15, 19]. This procedure refers to battery configuration of succes-

* To whom all correspondence should be sent:
E-mail: dalkaine@dq.ufscar.br

sive plates: positive-separator-negative-separator-positive-etc., with positive and negative plate ensembles. For this kind of configuration, several papers attribute the measured impedance to one of the ensembles [14–17]. Nevertheless, it has not been demonstrated experimentally that the total impedance can be attributed only to one plate ensemble. This is true even having one of the ensembles one plate in excess. On the other hand, if in this configuration the system is discharged, the two ensembles of plates will be discharged, in general, under different conditions and the external plate working solution will be depleted during the discharge. This last problem is not solved by waiting for some time to come to the rest potential, before the EIS measurement.

To solve the problem of two ensembles of plates (positive and negative), there are papers that reduce the configurations only to negative-separator-positive(central)-separator-negative (NspsN) or positive-separator-negative(central)-separator-positive (PsnsP) ensembles [19–21]. These configurations, depending on the cell dimensions and waiting time before EIS measurements, can have or not variation of external solution concentration when the system is discharged or charged. Beside this, in these systems the problem of attributing the total impedance to central plate, as stated in references [19–21], has not been experimentally demonstrated. Is the introduction of two counter-electrode plates enough to disregard their impedance contributions? A more difficult problem is the case NspsN configurations, because the BET surface area of positive active mass can be 10 to 20 times higher than the negative one [22]. This problem also affects studies without separators, where the cell has negative-positive-negative (NpN) configuration, like in references [23, 24], or positive-negative-positive (PnP) configuration. Nevertheless, these kinds of configurations are nearer to the traditional form to do EIS measurements.

The EIS measurements in the literature, with the pointed out problems, have also been made at different states of charge or discharge, in general, considering they can be referred only to the central plate. These measurements have been made during charge or discharge [17], sometimes, after stopping charge or discharge and waiting [23].

Nevertheless, it is possible to point out for all these kinds of configurations that all literature results present common patterns. In general, for NspsN or PsnsP or NpN or PnP configurations or even batteries, EIS results can be presented in Nyquist plots: a) an inductive loop at high frequencies; b) at least, as a minimum, a capacity loop at middle and low frequencies and c) even a new inductive loop at very low frequencies. Some papers [21] have found this last very low frequency inductive loop during intermediate states of discharge. Sometimes, these components do not appear, depending on the kind of plates, measurement cell characteristics, ways to obtain EIS data, used frequencies range and state of discharge (or charge). Finally, total charged systems seem to have particular behaviour [24], at least for NpN configuration.

The problem to disregard the counter-electrode plate contributions in a four electrode plate cell (a central working plate electrode, two lateral counter-electrode plates of opposite polarity and a reference electrode) will be central objective in the present work. To do that, external solution concentration will be maintained constant and counter-electrode plate surface area will be varied, maintaining the central working plate electrode at the geometrical centre of the ensemble. The work results, if they really give the central working plate impedance, will permit us to state with certainty, which are the real EIS results for negative (in PnP configuration) and positive (in NpN configuration) plates, at constant external concentrations and different states of discharge.

EXPERIMENTAL

The used experimental set-up was a four-electrode configuration (a working central plate electrode, two lateral plate counter-electrode and a reference one) shown in Fig. 1a for the discharge cell of the central plate and in Fig. 1b, for the EIS measurement cell. These permit two configurations for the EIS measurement cell, the positive-negative-positive one (PnP) and the negative-positive-negative one (NpN), which will be referred to in all the discussions. In the measurement cell the counter-electrodes were of variable area with the central electrode always in the centre of them. The distances between the lateral counter-electrodes and the central one were 3 cm in both cells, to maintain the external solution concentration constant in the discharge cell and to be able to place and to remove the central electrode in both cells. The cell solutions were always 4.6 M H_2SO_4 and the reference electrodes always $Hg/Hg_2SO_4/4.6$ M H_2SO_4, in regard to which all potentials will be given. The reference electrodes in both cells were always located near the central working one (see Figures 1a and 1b).
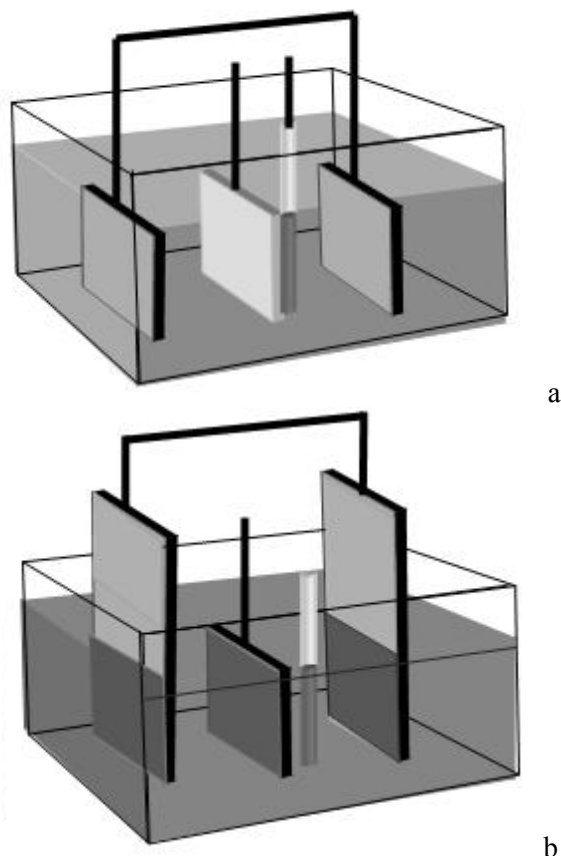
Fig. 1. Four electrode configuration with a central working plate, two lateral counter-electrode plates and a reference electrode. (a) Charge and discharge cell; (b) EIS measurement cell with variable counter-electrode area.

The electrode plates were real battery plates, removed from stationary batteries of two different sizes. The central electrodes were removed from a 12 Ah/6 Volts VRLA battery and the counter electrodes from a 600 Ah/2 Volts VRLA battery. All measurements, in the discharge and the EIS measurement cells, were made using the same central working electrode plate and counter-electrodes. The use of the same central plate was made because different plates can give slightly different data, which fact does not affect the results.

The central negative or positive working electrode plate dimensions were 4.4×6.6 cm (geometrical area about 60 cm^2 double face). Their real capacities, after stabilization, were 2.6 Ah for the negative plate electrode and 3.0 Ah for the positive one, in C_{20} discharge rates. These values will be used to calculate the state of discharge given in percentages, Q_d. The Q_d is in regard to the above real capacities. For the discharge cell, the counter-electrode plates had the same central working plate dimensions (see Fig. 1a) and they were always initially fully charged. On the other hand, counter-

electrode dimensions for EIS measuring cell were 14.0×20.0 cm (total geometrical area 280 cm^2 single face), always with the same width (14.0 cm) and initially fully charged. To vary counter-electrode area in the EIS measurement cell, these counter-electrode plates were partially immersed at different depth (see Fig. 1b). This gives rise to counter-electrode geometrical immersed single face areas of: a) 45 cm^2 (14.0×3.2 cm), b) 110 cm^2 (14.0×7.9 cm) and c) 205 cm^2 (14.0×4.6 cm). The different area ratios between counter-electrodes and central plates (single areas), called r, will be expressed as 1.5/1.0, 3.7/1.0 and 6.8/1.0, respectively. For measurements and discussions, these last values will be used. The positive real counter-electrode capacity, totally immersed, was 25 Ah at a C_{20} rate and that of the negative one, 22 Ah. The central working plates were always fully immersed and located, as near as possible, in the centre of the two counter-electrode immersed areas.

In the discharge cell, the partial or total discharges of the central plate were performed galvanostatically. For central negative plates the current density was 2.5 mA·cm^{-2} (double face), at C_{17} discharge rate. For positive central plates this current density also was 2.5 mA·cm^{-2} (double face), at a C_{20} discharge rate. In cases of total state of discharge, the cutting potential was up to –0.70 V for central negative plates and 1.05 V for the central positive plates.

To perform the impedance measurements, the central electrode at a given state of discharge was removed, each time, from the discharge cell (Fig. 1a) and immersed into the EIS measurement cell (Fig. 1b) with a given r.

The EIS data were obtained in different states of discharge using a Gamry Impedance System. The EIS galvanostatic measurements were made at the rest reversible potential (zero continuous current) and only after two hours of immersion in the measurement cell, at open circuit potential. A sinusoidal perturbation of 1 mA rms amplitude was used, in the linear region, with a frequency range from 10^4 to 10^{-2} Hz and 10 points per decade.

RESULTS AND DISCUSSIONS

Taking into account that BET negative plate surface areas are about 0.5 m^2·g^{-1}, while those of positive plate can be from 5 to 10 m^2·g^{-1}, we shall be firstly analyzed data from PnP configuration. This configuration can be considered as having enough real area ratio r, between counter and working electrodes. On the other hand, data from NpN configuration could have area ratio problems.

This is why it will be discussed later. The problem is the geometrical counter-electrode area duplication (which does not mean real area duplication) that could be not enough, in NpN configuration. A high real area ratio *r* permits to disregard, in EIS measurements, counter-electrode impedance contribution. In both cases, PnP and NpN configurations, the analysis will begin with completely charged and discharged working electrode plates (central plates), discharged up to the cutting potential. Finally, changes on the polarization resistances of found capacity loops at different state of discharge of both configurations will be discussed.

The PnP configuration

In Fig. 2 EIS results are plotted of the PnP configuration with totally charged and discharged working plates, for different *r* values. For *r* 3.7/1.0, the working electrode was over discharged beyond the cutting potential, to show that for negative plate the impedance module in these states of discharge becomes very much larger. This must be related to the fact that new products are formed on electrode pore surface. This does not happen in the case of positive plate, showing that negative and positive plates have different behaviors even when, in general, it is considered that they give as discharge final product the same material: insoluble $PbSO_4$.

A second point observable in Fig. 2 is that, as expected for PnP configuration at the different *r* values, the charged or totally discharged plates, give

the same Nyquist's plot. These results show that there is no *Z* dependence on *r*. The *Z* independence on *r* shows that the counter-electrode impedance can be disregarded. Nevertheless, there is an exception for highest *r* of charged plates. The explanation of 6.8/1.0 *r* value can be related to the existence of a non-uniform current distribution at the central plate, due to its specific geometrical configuration. To consider that the 6.8/1.0 result is the correct one is wrong. This is because it is incompatible with the other *r* values results.

A final point which arises from Fig. 2 is the fact that impedance imaginary components at the lowest measured frequency are equal inside the ensembles of charged or discharged negative plates. Nevertheless, the real component increases from charged to discharged plates, in agreement with the discharge growth. In connection with this fact, it must be taken into account that the impedances have been measured after 2 hours of stabilization in the measurement cell. In the charged cases, this implies auto-discharge reactions, producing very low discharge levels, which makes the charged and discharged electrodes not so different.

The EIS results for PnP configuration in intermediate states of discharge can be seen in Fig. 3 (Q_d 30%), Fig. 4 (Q_d 60%) and Fig. 5 (Q_d 90%). In all these figures, to compare the data for different *r* values, the serial resistance at high frequencies (R_s) for the highest *r* value was used as reference, shifting the other data. This was done at the respective inlets.
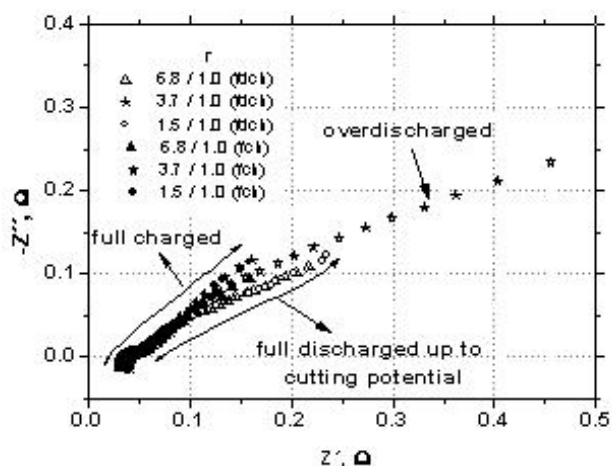

Fig. 2. PnP configuration EIS data under fully charged or fully discharged conditions, showing a case with central plate over discharge. Different *r* are pointed out in the figure. Fully charged: full symbols; fully discharged: open symbols.
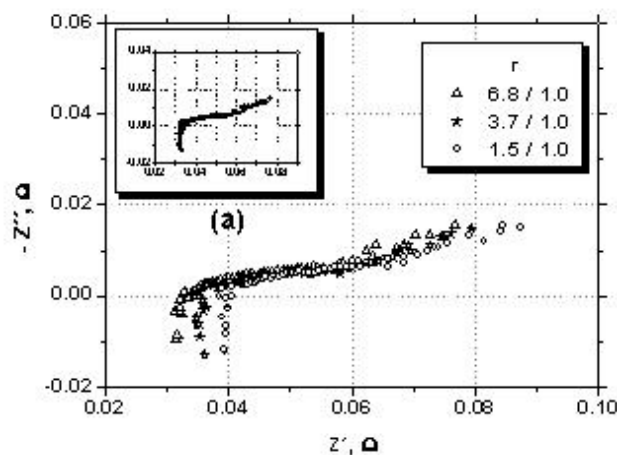

Fig. 3. PnP configuration EIS data for 30% state of discharge. Different *r* values pointed out in the figure. (a) Data shifting to coincide R_s at its lower value.
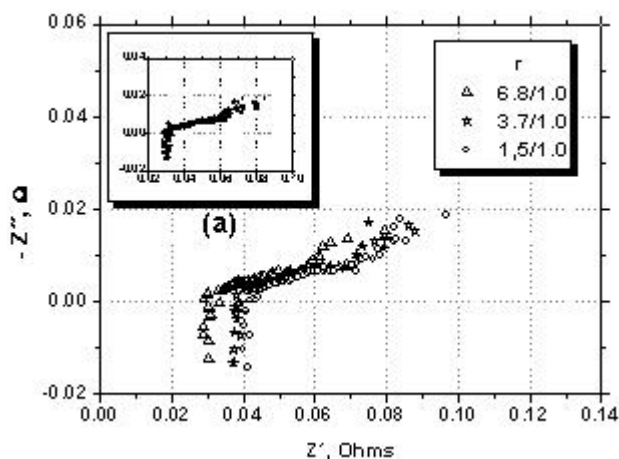
Fig. 4. PnP configuration EIS data for 60% state of discharge. Different *r* values pointed out in the figure. (a) Data shifting to coincide R_s at its lower value.
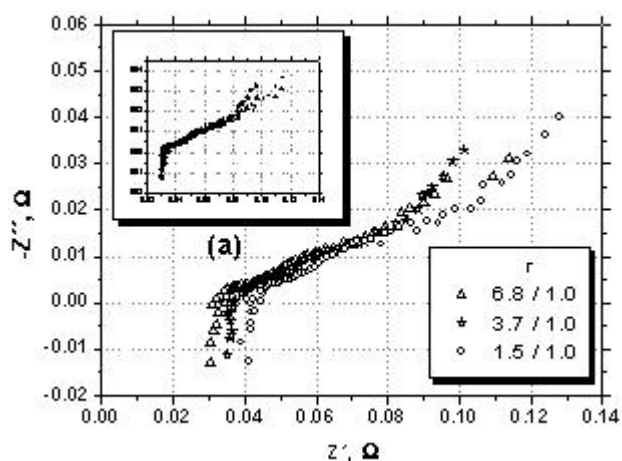

Fig. 5. PnP configuration EIS data for 90% state of discharge. Different *r* values pointed out in the figure. (a) Data shifting to coincide R_s at its lower value.

It is important to point out that R_s´s and, as a consequence, the differences between them are the same at each *r* in the three figures (the last ones giving approximately 0.032 Ω for 6.8/1.0, 0.035 Ω for 3.7/1.0 and 0.040 Ω for 1.5/1.0, with an error of ± 0.001 Ω). These differences agree quite well with theoretical calculations for different *r* values for the differences in solution resistances.

Figs. 3 and 4 show after shifting (see the inlets) that the data overlap for different *r*. This means that, in agreement with Fig. 2, the *Z* of the counter-electrode can correctly be disregarded. On the other hand, when discharge progresses, the real and imaginary *Z* components observed at the inlets, for the lowest frequency, practically do not grow (approximately, Z_{im} of 0.018 Ω and Z_{real} of 0.08 Ω). This fact is in agreement with the idea that the discharge reaction follows a zone reaction pattern [25].

When these data are compared with those at 90% of discharge, Fig. 5, a new aspect appears: the impedance differences for all the *r* ratios at low frequencies (see the inlet). It is like as if, with the reaction zone arriving to the end of plate pores a non-uniform current distribution appears influencing impedance measurements. The fact is interesting because in the evolution from Q_d 90% to 100% (total state of discharge), this situation disappears, as it is seen in Fig. 2. The supposition to accept as explanation of the above facts that the value of counter-electrode impedance cannot be disregarded, is incorrect. This is because the measured impedance has grown in view of Figs. 3 and 4 and the phenomenon occurs only at low frequencies. It is important to note that all these facts are totally reproducible with a given plate.

The NpN configuration

In Fig. 6, equivalent data to those in Fig. 2 are shown for NpN configurations. For this configuration, the two sets of data, for charged and discharged conditions, present problems in EIS measurements. This is because for both cases the impedance depends on *r*, for any value of this parameter. This is indicating that, in principle, counter-electrode impedance cannot be disregarded at least for *r* 1.5/1.0 and 3.7/1.0. The data for 6.8/1.0 must not be considered because it looks like presence of current distribution problems. All these are in agreement with the BET area ratios for negative and positive plates. Nevertheless, even considering that the central plate true impedance is not attainable, it is interesting to point out that in all these cases there is an important growth of the imaginary and real impedance components from charged to discharged central plates. This can be clearly seen at the lowest frequency. Here the impedance measurements under charged conditions were also made after sufficient waiting time during which some discharge can occur. These data are pointing out the differences in positive and negative plate behaviors in relation to discharge process, even when it is considered in the literature that both give the same final product: insoluble $PbSO_4$.
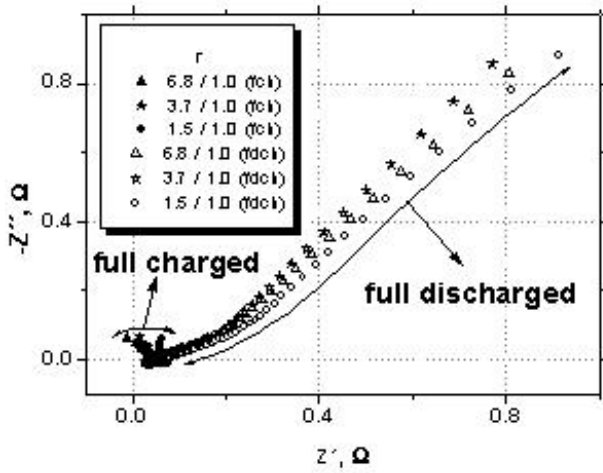
Fig. 6. NpN configuration EIS data under fully charged or fully discharged conditions. Different *r* values pointed out in the figure. Fully charged: full symbols; fully discharged: open symbols.
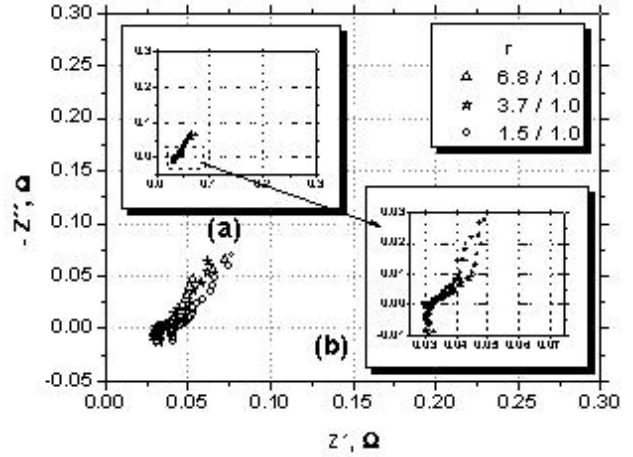

Fig. 7. NpN configuration EIS data for 20% state of discharge. Different *r* values pointed out in the figure. (a) Data shifting to coincide R_s at its lower value. (b) Magnification of inlet (a) region .
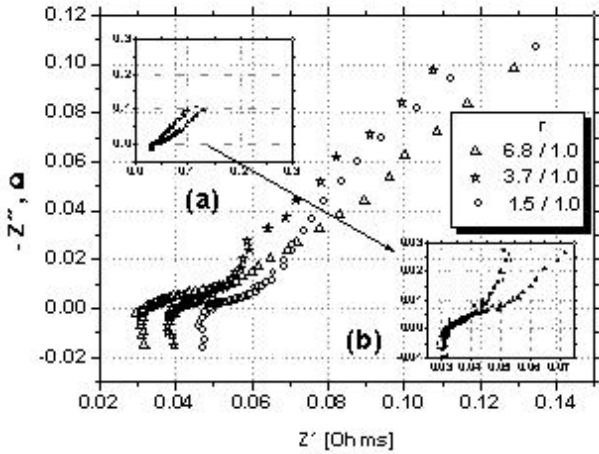

Fig. 8. NpN configuration EIS data for 40% state of discharge. Different *r* values pointed out in the figure. (a) Data shifting to coincide R_s at its lower value. (b) Magnification of inlet (a) region .
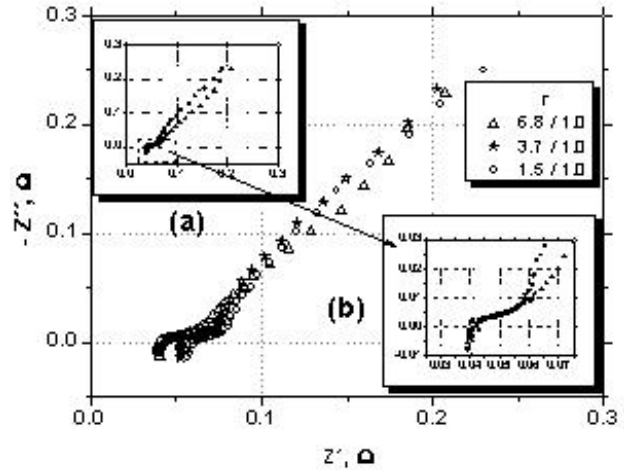

Fig. 9. NpN configuration EIS data for 80% state of discharged. Different *r* values pointed out in the figure. (a) Data shifting to coincide R_s at its lower value. (b) Magnification of inlet (a) region .

Another fact to be noted, because it is totally reproducible, is related to the discharge EIS plate data in Fig. 6 from 1.5/1.0 to 3.7/1.0, where there is a shift to the left in the figure. This is in agreement with the lower solution external resistance of the second case. Nevertheless, the data at *r* 6.8/1.0 seem to cross the others (this crossing is observable between 6.8/1.0 and 3.7/1.0, even without shifting the data). It is like the data from 1.5/1.0 to 3.7/1.0, which were "well" ordered (in some agreement with the external solution resistances). On the other hand, the data for 6.8/1.0 present "good" behaviour at high and middle frequencies, but problems at low frequencies. These problems can be interpreted in terms of a non-homogeneous current distribution, as it was previously supposed for other cases (Figs. 2 and 5).

The data with NpN configurations for partial discharged central positive plates are plotted in Figs. 7 (Q_d 20%), 8 (Q_d 40%) and 9 (Q_d 80%). In all these cases it is possible to see, looking at the respective inlets (which have the shifted data), that 1.5/1.0 and 3.7/1.0 ratios give always the same impedance behaviours. The *r* 6.8/1.0 presents for all cases and only at low frequencies a difference: a shifting to the right (see the inlets). At high and medium frequencies all the data coincide at the inlets. This means that the data under intermediate discharge conditions can be attributed to central positive plate impedance at high and middle frequencies. At low frequencies, increasing them with the discharge level, the data depend on *r*. This fact is in the sense that under these conditions (high discharge level and low

frequencies) there is a non-homogeneous current distribution interfering in the measurements. It is interesting that, under completely discharged conditions, the non-homogeneous current distribution becomes observable at all frequencies (see Fig. 6).

A last point in Figs 7, 8 and 9 is that, looking at observed impedance module for 1.5/1.0 and 3.7/1.0 ratios at the lowest frequency, they are practically constant from Fig 7 (Q_d 20%) to Fig. 8 (Q_d 40%). Nevertheless, there is an increase of module from Fig. 8 (Q_d 40%) to Fig. 9 (Q_d 80%). This gives another experimental basis to the idea that this last increase is related to the reaction zone reaching the bottom of the pores.

Analysis of polarization resistances versus discharge conditions

As it has been concluded in the two previous sections, it seems that the impedance measurements made in different states of discharge can be attributed only to the central plate impedance. Nevertheless, this statement is incorrect because of: a) the totally charged negative plates for r 6.8/1.0 (Fig. 2); b) the negative plate at high degree of discharge for r 6.8/1.0 and very low frequencies (Fig. 5); c) the positive plates at medium and high degree of discharge for r 6.8/1.0, at low frequencies (Figs. 8 and 9) and d) the totally charged or discharged positive plates at all the analyzed frequencies (Fig. 6). As a consequence, it can be stated that the data at r 1.5/1.0 are representative of the impedance of all central plates except for: i) totally charged or discharged NpN configurations; ii) positive partially charged plates, at low frequencies and iii) negative plates near to the end of the discharge, at low frequencies.

In all first three cases (a, b, and c), it seems that the phenomenon can be attributed not to an incorrect area ratio, but to a non-homogeneous current distribution at the central plate. Case d) (Fig. 6) seems to be related to PbO_2 electrode specific characteristics, together with its discharge product, both detected by the EIS method. These facts point out that the positive plate discharge product is different from that formed in negative plates [25].

The present EIS results on partially or totally discharged plates show an inductive loop at high frequencies and two capacities distributed loops, at middle and low frequencies. These ideas have been schematically represented in Fig. 10, together with some parameters used in the literature like R_s, Ω and R_{p2} [19]. In the present work it was possible to determine the polarization resistances $R_{p,1}$ and $R_{p,2}$ (see Fig. 10) in different states of discharge. They could be attributed to processes occurring on the

surfaces of two different kinds of pores. The idea about two kinds of pores comes from the measurements of Hg porosimeter and BET surface areas, which give different results. The $R_{p,1}$ and $R_{p,2}$ results seem to be a polarization resistance of the processes on the surfaces of these two kind of pores. In this sense, it is interesting to plot the results of these two parameters ($R_{p,1}$ and $R_{p,2}$) for PnP and NpN configurations, against the plate state of discharge. To do that, the determination of $R_{p,1}$ and $R_{p,2}$ was made by non linear fitting of the points, considering only those from a single capacity loop.
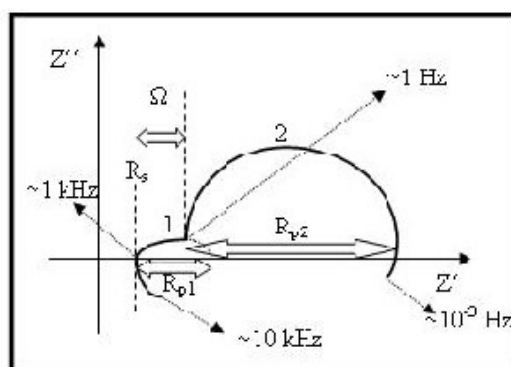

Fig. 10. Schematic representation of EIS lead acid battery plates results including all the observed phenomena in partial or totally discharged plates.

In Fig. 11 $R_{p,1}$ and $R_{p,2}$ are plotted results versus discharge levels for PnP configuration and, in Fig. 12, those for NpN configuration. The first important aspect is that both results are coherent in themselves, because they give rise to continuous curves for each case. A second point is that for both cases the $R_{p,1}$ seems to be independent of the state of discharge, except for the NpN configuration at high discharge level. In this region, there is a little increase of $R_{p,1}$. The average value of $R_{p,1}$ for the PnP configuration (related to negative central plate) was 46 ± 7 mΩ and that of NpN configuration, taking out the high discharge levels, was 24 ± 6 mΩ.
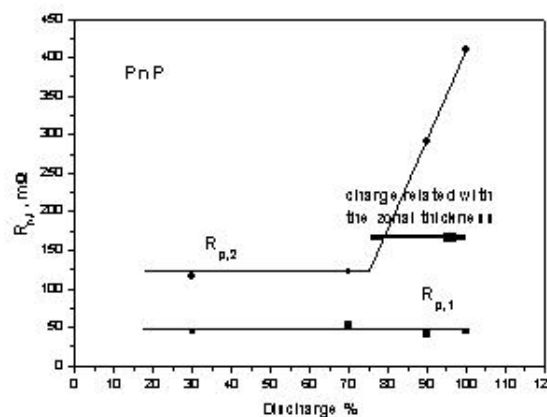

Fig. 11. $R_{p,1}$ and $R_{p,2}$ versus discharge percentage (state of discharge) plot for a PnP configuration.
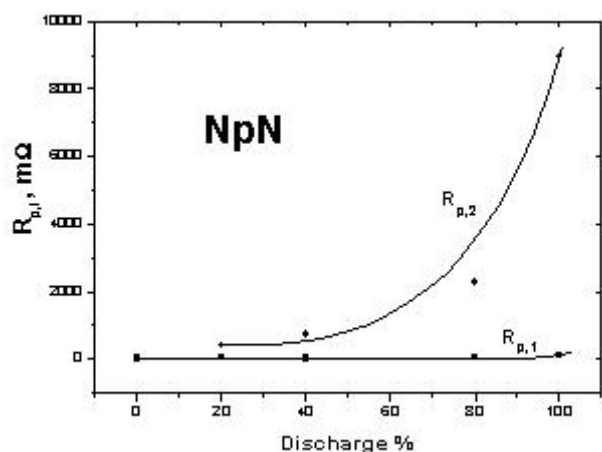
Fig. 12. $R_{p,1}$ and $R_{p,2}$ versus discharge percentage (state of discharge) plot for a NpN configuration.

On the other hand, the $R_{p,2}$ results are different for PnP and NpN configurations. In PnP configuration cases, considering the determined $R_{p,2}$ value as due only to negative central plate, there is a drastic change of behaviour of the related process in about 80% state of discharge. It can be attributed to the fact that this drastic change occurs, when the discharge reaction zone reaches the bottom of the pores measured, indirectly, through BET. For the NpN configuration results (considering now the $R_{p,2}$ related only to the positive central plate), they seem to have a more extended reaction zone, which makes impossible to detect clearly the reaching of the discharge reaction zone to the bottom of BET pores.

Pointing out that the determined $R_{p,1}$ and $R_{p,2}$ results are reproducible, these two concepts can give base to be used in understanding other systems, which have behaviour like those schematically represented in Fig. 10. In this sense, it is interesting to note that $R_{p,1}$ is higher in negative than positive plates, while $R_{p,2}$ has an opposite behavior for the same states of discharge. These last facts need to be more deeply studied in different lead acid battery systems.

CONCLUSIONS

On the basis of the fact that in the literature for EIS measurements in different kinds of four electrodes cells, there are no experimental proofs that the total measured impedance can be attributed only to the central plate studies were made in the present work, to clarify experimentally the problem. The four-electrode cells use lead acid battery plates as central electrode and lateral counter-electrodes with different polarity, plus a reference one. Literature sources consider the two counter-electrodes presence enough to resolve the counter-electrode impedance problem.

To perform these studies on plates a special four electrode EIS measurement cell was developed, to be able to vary the counter-electrode plate area at the same time when the central working plate area was maintained constant. The central plate was located geometrically at the centre of two counter-electrodes and at 3 cm distance from them. This last prerequisite was established to assure, so far as possible, that the increase in the counter-electrode areas does not introduce increasing currents at central plate borders. This cell was used under two configurations, PnP and NpN (see the text), with the central plate electrode in different states of discharge, and the reference electrode near to the central one. The used area ratios r between the counter-electrode and the central plate were 1.5/1.0, 3.7/1.0 and 6.8/1.0. For discharge cell an equivalent configuration but with r of 1.0 was used.

The results for the PnP configuration show that in these cases it was always possible to attribute the EIS measurements to the central negative plate, even for totally charged central plate. This does not occur only at lower used frequencies and higher degrees of discharge, where the EIS measurements become dependent on the r value. Nevertheless, in the present work there are arguments to attribute this fact to a current distribution problem at the central plate borders, and not to a specific counter-electrode contribution to the total impedances.

The results for NpN configuration are more complicated. In these cases (NpN) it can be stated that at high and middle frequencies the measured impedance can be attributed to the central plates, except for totally charged plates where it depends on r. On the other hand, at low frequencies, in all these cases (state of discharge, different r and even totally charged plates) there are dependences on the r values. Nevertheless, again, arguments are put forward in the sense that this dependence could not be related to counter-electrode impedance contributions, but to central plate current distribution problems. In this sense, it becomes an open problem, to which point non-homogeneous distribution of a.c. current densities. Perturbations can invalidate impedance measurements.

REFERENCES

1. R. de Levie, *Electrochim. Acta*, **8**, 751 (1963).
2. H. Keiser, K. D. Beccu, M. A. Gutjahr, *Electrochim. Acta*, **21**, 539 (1976).
3. W. H. Mulder, J. H. Sluyters, T. Pajkossy, L. Nyikos, *J. Electroanal. Chem.*, **285**, 103 (1990).
4. A. Lasia, *J. Electroanal. Chem.*, **397**, 103 (1995).
5. A. Lasia, *J. Electroanal. Chem.*, **428**, 155 (1997.
6. R. de Levie, *Electrochim. Acta*, **10**, 113 (1965).
7. D. D. Macdonald, *Electrochim. Acta*, **51**, 1376 (2006).
8. J-P. Candt, P. Fouilloux, M. Keddam, H. Takenouti, *Electrochim. Acta*, **26**, 1029 (1981).
9. D. D. Macdonald, M. Uriquidi-Macdonald, S. D. Bhakta, B. G. Pound, *J. Electrochem. Soc.*, **138**, 1359 (1991).
10. E. Karden, S. Buller, R. W. De Doncker, *Electrochim. Acta*, **47**, 2347 (2002).
11. S. Devan, V. R. Subramanian, R. E. White, *J. Electrochem. Soc.*, **152**, A947 (2005).
12. F. La Mantia, J. Vetter, P. Novak, *Electrochim. Acta*, **53**, 4109 (2008).
13. A. L. Van Den Eeden, J. H. Sluyters, J. H. Van Lenthe, *J. Electroanal. Chem.*, **171**, 195 (1984); A. L. Van Den Eeden, Thesis, Utrecht University, 1955, pp. 78-79.
14. F. Huet; *J. Power Sources*, **70**, 59 (1998}.
15. M. Keddam, Z. Stoynov, H. Takenouti, *J. Appl. Electrochem.*, **7**, 539 (1977).
16. V. V. Viswanathan, A. J. Salkind, J. J. Kelleo, J. B. Ockerman, *J. Appl. Electrochem.*, **25**, 729 (1995).
17. F. Huet, R. P. Nogueira, P. Lailler, L. Torcheux, *J. Power Sources,* **158**, 1012 (2006).
18. E. Karden, S. Uller, R. W. De Doncker, *J. Power Sources*, **85**, 72 (2000).
19. M. Keddam, C. Rakotomavo, H. Takenouti, in: Advances in Lead-Acid Batteries, K. R. Bullock, D. Pavlov (Eds.), The Electrochemical Society Inc., Pennington, N.J., USA, 1984, p. 277.
20. J. Jindra, M. Musilová, J. Mhra, A. A. Taganova*, J. Power Sources*, **37**, 403 (1992).
21. Z. Stoynov, B. Savova-Stoynov, T. Kossev, *J. Power Sources*, **30**, 275 (1990).
22. D. Berndt, Maintenance-Free Batteries, A Handbook of Battery Technology, Research Studies Press Ltd., Baldock, Hertfordshire, England, 2003, p. 262.
23. A. Kirchev, A. Delaille, M. Perrin, E. Lemaire, F. Mattera, *J. Power Sources*, **170**, 495 (2007).
24. A. Kirchev, A. Delaille, F. Karoui, M. Perrin, E. Lemaire, F. Mattera, *J. Power Sources*, **179**, 808 (2008).
25. C. V. D'Alkaine, A. Carubelli, M. C. Lopes, *J. Power Sources*, **64**, 111 (1997).

ЕКСПЕРИМЕНТАЛЕН КРИТИЧЕН АНАЛИЗ НА ИМПЕДАНС НА АКУМУЛАТОРНИ ПЛОЧИ

С. В. Д'Алкаине[1]*, Г. А. де Оливейра Брито[1], К. М. Гарсия[2], П. Р. Импиниси[2]

[1] *Група по електрохимия и полимери, Химически департамент, Федерален университет на Соа Карлос, бул. „Вашингтон Луиз" 234, 13560-905 Сао Карлос, Бразилия*
[2] *Лаборатория по батерии, Институт по технологии за развитие, Политехнически център, ПК 19067, 81531-980 Куритиба, Бразилия*

(Резюме)

Отчитайки отсъствието на експериментални доказателства за това, че измерванията на клетка с четири плочи чрез електрохимичната импедансна спектроскопия (ЕИС) се свързват само с централната плоча, в настоящата работа са проведени изследвания с различни по площ плочи на противоелектрода при една и съща централна плоча. Измерванията са проведени в честотната област от 10^4 до 10^{-2} Hz при различна степен на зареждане на централната плоча. Резултатите показват, че за комбинацията положителна-отрицателна-положителна плоча при всички изследвани честоти и състояние на разреденост данните от ЕИС могат да бъдат отнесени за централната отрицателна плоча, освен при най-голямо отношение на площите *r* сравнителен електрод/централен работен електрод и по-висока степен на разреждане в зоната на по-ниските работни честоти. За комбинацията отрицателен-положителен електрод резултатите от ЕИС могат да бъдат отнесени към централната положителна плоча само за високи и средни честоти при всички нива на разряд и отношения на площите. Напълно заредените централни положителни плочи трябва да бъдат изключени, защото техният импеданс зависи от площта на противоелектрода при всички съотношения *r*. Резултатите са обсъдени и са направени предположения за тяхното обяснение.